ORIGINAL ARTICLE

Modeling canopy photosynthesis and light interception partitioning among shoots in bi-axis and single-axis apple trees (*Malus domestica* Borkh.)

Weiwei Yang[1,2] · Xiaolong Ma[1] · Doudou Ma[1] · Jidong Shi[3] · Sayed Hussain[5] · Mingyu Han[1] · Evelyne Costes[4] · Dong Zhang[1]

Key message **Bi-axis training increased vegetative shoot light interception and modeled photosynthetic rate, and reduced fruiting shoot mutual shading and vegetative growth by optimizing canopy structure compared to single-axis in young apple trees.**

Abstract Improving light interception and distribution within canopy are constant objectives of training through manipulating tree architecture. A bi-axis training system with two primary scaffolds has been proposed to improve flowering and dry matter production in apple trees. In this study, 'Fuji' apple trees trained using a bi-axis or single-axis training system were compared. Twelve three-dimensional (3D) virtual apple trees were reconstructed by combining 3D digitizing and allometric relationships for three shoot types (vegetative long shoot, VL; fruiting shoot, FS; vegetative short shoot, VS), to evaluate canopy structure impacts on light interception. Light interception efficiency was evaluated by silhouette to total area ratio (STAR). The potential canopy photosynthetic rate was evaluated by the eco-physiological RATP model. The leaf area of VL in bi-axis trained trees was approximately 40% lower than that in single-axis trees. Lower leaf area and more uniform spatial distribution were noted in VL in bi-axis than in single-axis trees. This led to more even spatial light distribution and more shoots having higher STAR in bi-axis than in single-axis trees, regardless of the whole tree or shoot type. In the virtual orchard, bi-axis trees had a 25% and 10% STAR increase in VS and VL, respectively, but a similar STAR for FS compared to single-axis trees. Mutual shading between neighboring trees in the virtual orchard made of bi-axis trees was significantly lower than that with single-axis trees for FS. The modeled canopy net photosynthetic rate was 26% higher in bi-axis than in single-axis trees. With the increase in tree age, the projected leaf area increased, but the porosity of the canopy decreased, and mutual shading increased for the whole canopy and all shoot types, irrespective of training systems. These results indicated that manipulating scaffolds in apple trees can regulate canopy structure, light interception, and vegetative growth during the early developmental stages.

Keywords 3D digitizing · Virtual orchard · STAR · Mutual shading · Training system · Fruiting shoot · Vegetative shoot

---

Weiwei Yang and Xiaolong Ma contributed equally to this work.

Mingyu Han: Deceased on 2nd August 2018.

✉ Dong Zhang
afant@nwsuaf.edu.cn

Extended author information available on the last page of the article

Introduction

Improving the light environment within a complex fruit tree canopy has always been of great practical interest for enhancing fruit yield and quality (Jackson 1980; Wunsche and Lakso 2000; Coupel-Ledru et al. 2019). Plant architecture, i.e., the topological arrangement of branching and successive growth as well as geometrical attributes of plant components, determines the spatial light distribution and interception within the canopy (Costes et al. 2006; Barthélémy and Caraglio 2007). The resulting heterogeneous light distribution within the canopy mediates microclimate and organ activities by energy exchange with the

surrounding environment, at both organ and canopy scales (Niinemets 2010; Gullo et al. 2014; Poorter et al. 2019). For instance, changes in the amount of intercepted light by organs can modify the leaf nitrogen spatial distribution, leaf transpiration (Giuliani et al. 1998; Larbi et al. 2015), carbon assimilation and allocation (van Hooijdonk et al. 2015; Afonso et al. 2017), as well as flowering, fruit production, and composition (Hampson et al. 2002; Feng et al. 2014). Moreover, light affects pathogen attacks, development, and spatial distribution within the canopy (Costes et al. 2013).

Several architectural traits have previously been confirmed to alter the light environment, notably leaf area density (LAD) (Wagenmakers and Callesen 1995), internode length (Han et al. 2012), and branching patterns (Da Silva et al. 2013; Tang et al. 2019). However, tree architectural characteristics were seldom considered in long-term breeding programs compared to disease resistance, fruit yield, and quality (Laurens et al. 2018). Orchard managers around the world conventionally manipulate apple tree canopies via training, pruning, bending, and leaf removal to optimize the light penetration into canopy and fruit attributes to obtain desired quality standards (Jackson 1980; Robinson and Lakso 1991; Li et al. 2003; Stephan et al. 2008; Xing et al. 2016). Based on those studies, canopy manipulations not only balance light interception and distribution within canopy (Corelli-Grappadelli and Lakso 2007), but also allow an adequate amount of light to reach the fruiting shoot leaves to obtain high-quality fruits (Willaume et al. 2004; Fanwoua et al. 2014). Furthermore, dwarfing rootstocks by reducing the tree size and increasing planting density have been shown to efficiently improve light utilization in orchards (Yang et al. 2016, Buler et al. 2001). In high-density orchards with dwarfing rootstocks, the tall spindle has become the predominant and most profitable training system in most areas of the world (Tustin et al. 1998; Lauri et al. 2004; Willaume et al. 2004; Robinson et al. 2007, 2013; Reig et al. 2019). Nevertheless, the inner central part of a single-axis tall spindle tree is not well illuminated, resulting in excessive annual vegetative growth on the exposed side of scaffolds and a reduced percentage of red-colored fruit (Palmer and Warrington 1998; Buler and Mika 2004; Yang et al. 2016; Reig et al. 2019). A training system called Bibaum®, based on bi-axis trees made of two primary scaffolds, was applied to apple and pear trees (Musacchi 2008a). It was reported to allow a higher leaf net photosynthesis rate and dry matter production than the tall spindle training system, presumably due to an early leaf area development that in turn increased the light interception (van Hooijdonk et al. 2015, 2016; Afonso et al. 2017). However, the impacts of bi-axis Bibaum® on the canopy structure, light interception, spatial distribution and partitioning at both tree and intra-tree scales, and on other canopy performances in terms of tree photosynthesis, transpiration, and water use efficiency have not yet been well elucidated.

Over the years, three-dimensional (3D) virtual plant modeling approaches have been successfully used to characterize canopy structures and light interception efficiency (Willaume et al. 2004; Stephan et al. 2008; Da Silva et al. 2014; Perez et al. 2019). In 3D virtual plants, the plant structure is represented in silico and its components are characterized by assigned geometric shapes with attributes, such as dimensions and spatial localization (Strauss et al. 2020). A virtual plant can be obtained by 3D digitizing (Sinoquet et al. 1997), terrestrial light detection and ranging (LiDAR) (Colaço et al. 2018), or by morphological and developmental rule-based simulations (Prusinkiewicz 1998). Three-dimensional digitizing remains time-consuming and is often limited to small plants and lower numbers of trees. Terrestrial LiDAR has emerged as a new phenotyping method to evaluate individual crown architecture (Coupel-Ledru et al. 2019) or LAD (Sanz et al. 2013), but it has a larger number of occlusions (Mack et al. 2017) and still poses some challenges. When terrestrial LiDAR was used on apple trees, the 3D reconstructions underestimated short shoots, which were the most numerous components of the canopy at the adult stage (Pallas et al. 2018). Rule-based simulation is also limited in generating complex plant structures, because it can be time-consuming to generate numerous trees in parallel at an orchard scale. Alternatively, partial 3D digitizing of a canopy, allometric relationships, and random distribution of certain organs attributes from fully digitized parts have been successively combined to reconstruct the 3D canopy structure (Sonohat et al. 2006). Thus, light interception efficiency can be precisely estimated for any organ or at any spatial scale based on the reconstructed canopy and is termed the silhouette to total area ratio (STAR) (Carter and Smith 1985). The STAR is considered the representation of light interception efficiency and can be used as a criterion to design an ideal canopy structure in fruit trees (Picheny et al. 2017; Tang et al. 2019). Furthermore, quantitative parameters have been proposed to evaluate the canopy structural properties, such as canopy volume (V), total leaf area (TLA), LAD and its variance (LAD_{var}), as well as light interception properties, such as the projected leaf area (PLA), projected envelope area (PEA), mean optical density (MOD), porosity (Po), and leaf dispersion (μ) (Sinoquet et al. 2005; Stephan et al. 2008; Duursma et al. 2012; Yang et al. 2016). Light interception properties are usually estimated from virtual trees under isolated conditions without surrounding trees (hereafter called isolated trees) during light modeling. However, the mutual shading effect, which strongly relates to planting density, needs to be considered.

According to the equation of Monteith (1977), in addition to light interception efficiency, yield also depends on the energy conversion efficiency, which is the ratio of biomass

produced over a given period through the photosynthetic process to the intercepted radiative energy of the canopy over the same period (Zhu et al. 2010). However, leaf photosynthetic capacity displays strong heterogeneity within the canopy. Therefore, whole canopy photosynthesis cannot be estimated from "an average leaf response" as it is the integrated response of leaves in different canopy positions with different physiological potentials tuned to their specific light environment (Hikosaka et al. 2016). Tackling such issue is an advantage of 3D virtual plants coupled with an eco-physiological model such as RATP that estimates the canopy net photosynthetic rate (Ac) and transpiration rate (Ec) (Sinoquet et al. 2001). RATP combines: (1) an intermediate 3D representation of a tree canopy with (2) a simulation of light interception integrated in all sky directions and (3) selected biophysical functions (energy balance and microclimate, such as temperature, wind speed, and vapor pressure deficit) with (4) stomatal conductance and photosynthesis sub-models (Farquhar et al. 1980; Harley et al. 1992). The model has been validated and applied to fruit trees to study the impact of tree structures on Ac, Ec and temperature, particularly in apple (Massonnet et al. 2008; Ngao et al. 2017; Woods et al. 2018).

To further understand bi-axis training system properties and impacts on the canopy structure and light interception, we trained 'Fuji' apple trees grafted onto the widely used dwarf M9-T337 rootstock in either a single- or bi-axis training system. For comparing those trees, 3D virtual plants based on digitizing were reconstructed, and canopy structure and light interception and distribution were estimated at both tree and intra-tree scale. The canopy daily Ac, Ec, and water use efficiency (WUEc) were estimated by the RATP model and compared between the two training systems.

Materials and methods

Plant materials

The experiment was carried out in a commercial apple orchard located 930 m above sea level, in Qianyang (34.62° N, 107.22° E), China. The average annual temperature, precipitation, frost-free days, and sunshine duration in the region are 11.8 °C, 532.5 mm, 197 days and 1983 h, respectively. Fully feathered nursery 'Fujiko' trees (2 years in the nursery) were used and planted in the spring season of the year 2015 and the experiment was conducted during the 4th and 5th year of tree growth. 'Fujiko' is a new apple variety that is characterized by an intense red color on the skin surface, selected from a block of the adjacent Fuji 'NAGAFU 12' trees (Leis and Mazzola 2008). During winter of the year 2012, scions were grafted with three buds onto the newly harvested, 1-year old M9-T337 rootstock at

a height of 35 cm and planted in the orchard in spring of 2013. After bud-break in the spring of 2013, scions were de-budded to leave either single or two primary axes per tree. Trees with one primary axis (single-axis) were trained according to the tall spindle training system (Robinson et al. 2008, 2006; van Hooijdonk et al. 2015). Trees with two primary axes (bi-axis) were trained according to the method based on Bibaum® (Musacchi 2008a, b). All the trees were planted in rows spaced 3.5 m apart, with 1 m within the row for single-axis and 1.2 m for bi-axis trees, in a north–south orientation. The horizontal distance between the two primary axes in bi-axis trees was 60 cm. Horticultural practices included drip irrigation for integral control of watering, fertilization, and phytosanitary treatments. There was no pruning during the experiment and the average fruit load was 3.96 ± 0.62 fruits per trunk cross-sectional area (cm^2) for the two training systems during the 2 years. The soil in orchard was a sandy loam. The contents of organic matter, total nitrogen, total phosphorus, and available potassium were 1.51 g kg^{-1}, 1.0 g kg^{-1}, 3.64×10^3 mg kg^{-1} and 159 mg kg^{-1}, respectively.

Tree digitizing and foliage reconstruction

Before harvest (mid-October), three trees per training system for 4-year-old trees in 2016 and for 5-year-old trees in 2017 were chosen for tree digitizing. The spatial coordinates of the distal and proximal points of all of the current-year leafy shoots were measured with 3SPACE FASTRAK using a Stylus receiver (Polhemus; Cochester, VT, USA) and recorded with PiafDigit software (Donès et al. 2006). This allowed the computation of shoot length and orientation. All the shoots of the trees were classified as floral shoots or vegetative shoots. A floral shoot is composed of a bourse (*B*) and bourse shoot(s). Vegetative and bourse shoots were divided into short and long shoot, marked as VS and VL, and BS and BL, respectively (Costes et al. 2006). A threshold of 5 cm was used to separate the long from the short shoots.

Then, 20–27 randomly selected shoots per shoot type were digitized both at leaf- and shoot-scale. After digitizing, shoot length, individual leaf area, leaf width, leaf length, petiole length, and the number of leaves were recorded for the sampled shoots. This allowed us to estimate the allometric relationships among the shoot length, shoot leaf area, and the number of leaves using the methods of Palmer (1987). We also estimated the allometric relationships among the leaf length, leaf width, leaf area, and petiole length. The leaf Euler angle (midrib azimuth and inclination, lamina rolling around the midrib) distribution and the angle between the petiole and shoot axis were measured according to Sonohat et al. (2006). All the leaf- and shoot-scale measurements were conducted on all shoot types, for both training systems. Since the collected leaf- and shoot-scale data during the year

2016 were lost due to hard-disk damage, only data collected in the year 2017 were available.

The 3D distribution of leaves associated with each shoot type within the canopy was reconstructed based on Sonohat et al. (2006) using the same leaf- and shoot-scale parameters estimated in 2017 (Table S1). The reconstructed 3D virtual trees had a database of leaves, including leaf spatial coordinates, leaf dimensions, orientation angles, shoot type, and associated colors (Fig. 1). In total, a database of 3 (replicates) × 2 (training systems) × 2 (years) trees was created.

Extracting canopy structure parameters of isolated trees

For each tree, canopy structure parameters were extracted from the reconstructed leaf database. Total leaf area (TLA) was estimated as the sum of individual leaf areas for the whole canopy and each shoot type. When fruit(s) settled on the bourse, the bourse and associated BS or BL were considered fruiting shoots (FS). Otherwise, the bourse and associated BS and BL without fruits were identified as VS

and VL based on length. Consequently, TLA for FS, VS and VL was computed.

The canopy volume (V) was estimated using a bounding box method by dividing the canopy into cubic voxels with 20-cm-long edges based on the 3D spatial coordinates of leaves. We counted and added the number of voxels containing at least one leaf to compute V. Canopy LAD was computed as the ratio of canopy TLA to V. The relative variance of leaf area density (LAD_{var}) was reported as a parameter indicating leaf clumping and was computed from the LAD of each voxel (LAD_v):

$$LAD_{var} = \frac{1}{n_v} \sum_{i=1}^{n_v} \frac{\left(LAD_v - LAD\right)^2}{LAD}, \tag{1}$$

where n_v is the number of voxels.

Then, 2D maps of LAD were drawn, with LAD as a function of tree height and distance to the tree trunk based on the divided voxels, according to Stephan et al. (2008). Maps were drawn for the whole tree and each shoot type.
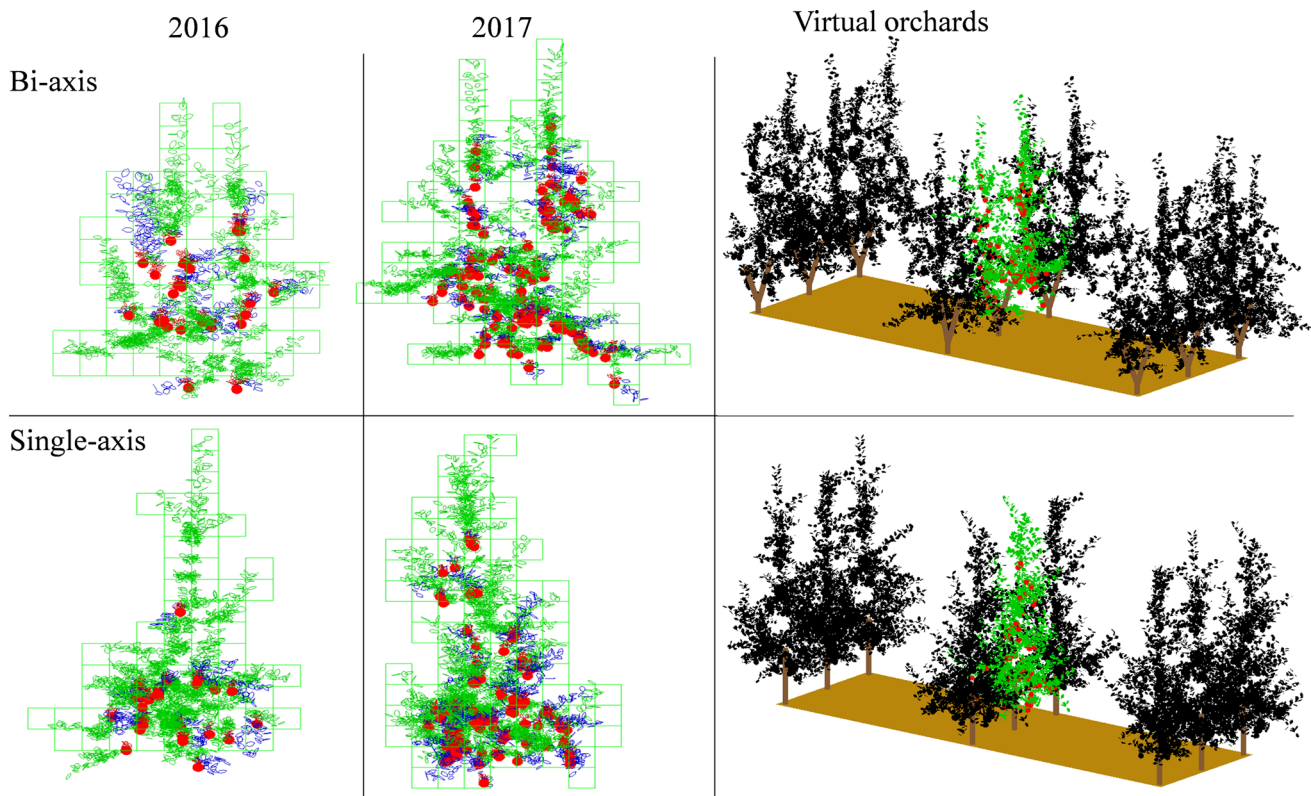
Fig. 1 Three-dimensional representation of reconstructed isolated 'Fuji' trees grafted on M9-T337 rootstock trained either with a bi- or single-axis training systems in 2016 and 2017, respectively. Canopy volume were divided by a set of voxels. Each voxel is a 0.2 m cube. False colors were assigned to shoot type: hexagons were leaves and spheres are fruits, red bourses; blue bourse shoots; green vegetative shoot. In virtual orchard, the central color tree was the target tree which silhouette to total area ratio (STAR) was computed in virtual orchard, the surrounding trees were given in a black color. Tree size can be estimated according to the number of voxels. Virtual images were synthesized with VegeSTAR4.0 software

Estimating light interception of isolated trees

The light interception of isolated trees was computed from isolated 3D virtual trees for whole trees and each shoot type based on the projected leaf area (PLAi) and TLA (Sinoquet et al. 2007) using VegeSTAR software (Adam et al. 2002). VegeSTAR computes the PLAi by processing the virtual images of 3D virtual trees. In a given light direction, a photograph was taken with an orthographic degree, and PLAi values were computed by counting vegetation pixels from the image, indicating the leaf area illuminated by light in a given sun direction. STARi represents the average leaf irradiance related to incident radiation and equals the ratio of PLAi to TLA. Both PLAi and STARi depend on the direction of incident light (Ω). Light interception was computed from 46 light directions over the sky vault, according to the Turtle sky model proposed by den Dulk (1989). Finally, the sky-integrated PLAi values were computed by averaging $PLAi_\Omega$ values using the weighted coefficients (W_Ω) derived from the standard overcast distribution of sky radiance (Moon et al. 1942) as follows:

$$PLAi = \sum_{\Omega=1}^{n} \left[PLAi_\Omega W_\Omega \right]. \tag{2}$$

The projected envelope area (PEA) was computed using VegeSTAR by replacing the leaves within the canopy with associated voxels. Then, the PEA was used to calculate Po and MOD as follows:

$$Po = 1 - PLAi/PEA, \tag{3}$$

and

$$MOD = TLA/PEA. \tag{4}$$

The MOD is similar to the LAI of an isolated tree. Leaves within the canopy were randomly distributed in the canopy volume defined by the voxels to produce a homogeneous canopy. Thus, the PLA of a homogeneous canopy ($PLAi_H$) and the porosity of a homogeneous canopy (Po_H) were computed as follows:

$$PO_H = 1 - PLAi_H/PEA, \tag{5}$$

Then, the leaf dispersion (μ) was computed according to Nilson (1971):

$$\mu = \ln Po / \ln PO_H, \tag{6}$$

where μ represents foliage clumping, and a μ value less than 1 means a clumped canopy. Similarly, 2D maps of light interception, as a function of tree height and distance to the trunk, were drawn by combining the method used for 2D maps of LAD for the whole tree and each type of shoot (VS, VL, and FS).

Estimation of light interception in virtual orchard

To consider and quantify the effect of neighboring trees on light interception in an orchard, in the virtual orchard, trees were 'planted' with the same planting density (1.2×3.5 m) and actual row orientation than in the field. First, a series of virtual orchards with different tree numbers were created to choose a suitable orchard. For a specific treatment, an isolated tree located at the coordinates of ($x = 0$, $y = 0$) was regarded as the central tree and a '1-tree orchard'. A positive x value indicated an easterly direction and a positive y value indicated a northerly direction. Then, the size of the virtual orchard was increased by adding randomly selected reconstructed trees from each associated category in a clockwise direction (Fig. S1). For example, the second tree was located at (3.5, 0 m) and the third at (3.5, − 1.2 m). Second, the STAR of each central tree was computed in a series of virtual orchards. Third, the most suitable virtual orchard size was determined according to the trend of STAR versus the size of the virtual orchard. STAR dramatically decreased from the "1-tree orchard" to the "8-tree orchard," then decreased slowly and reached a steady-state STAR varied within 5% when the number of trees in the virtual orchard reached 25 (Fig. S2). Finally, a reconstructed tree was planted in the center of its corresponding virtual orchard. Just as PLA was estimated from an isolated tree, the PLAo and STARo values for the central tree in the virtual orchard were estimated using VegeSTAR software. Accordingly, light mutual shading (Lms) results from neighboring trees in the orchard were computed, as follows:

$$Lms = (STARi - STARo)/STARi, \tag{7}$$

Additionally, for single-axis trees, STARo and Lms were estimated with a density of 1.0×3.5 m to allow us to analyze the effect of planting density on canopy light interception (Tables S2–3). All the acronyms for canopy structural and light interception traits are listed in Table 1.

Estimating photosynthesis, transpiration and water use efficiency of isolated canopy

The daily Ac and Ec of isolated canopy were estimated with RATP (Sinoquet et al. 2001), which is available in the OpenAlea platform (Pradal et al. 2008). Canopy WUEc was computed as the ratio of Ac to Ec.

The RATP inputs included meteorological datasets, leaf spatial distribution, and leaf physiological characteristics. In the present study, only the difference in the leaf spatial distribution resulting from different training systems was considered, the other inputs between training systems were identical. In the RATP model, leaf spatial distribution was

Table 1 Summary of acronyms for canopy architectural and light interception traits

Variable	Description	Units
Estimated from isolated trees		
V	Canopy volume estimated by bounding box	m^3
TLA	Total leaf area	m^2
LAD	Leaf area density estimated as leaf area to V ratio	$m^2\,m^{-3}$
LADvar	Relative variance of leaf area density estimated with Eq. (1)	
PLAi	Projected leaf area estimated with Eq. (2)	m^2
STARi	Silhouette to total area ratio estimated as ratio of plai to TLA	
Po	Canopy porosity estimated with Eq. (3)	
MOD	Mean optical density estimated with Eq. (4)	$m^2\,m^{-2}$
PEA	Projected envelope area	m^2
$PLAi_H$	Projected leaf area estimated with Eq. (2) from homogeneous canopy	m^2
Po_H	Canopy porosity estimated with Eq. (5)	
μ	Leaf dispersion estimated with Eq. (6)	
Estimated from trees in virtual orchard		
PLAo	Projected leaf area estimated with Eq. (2)	m^2
STARo	Silhouette to total area ratio estimated as ratio of plao to TLA	
Lms	Light mutual shading estimated with Eq. (7)	

estimated from reconstructed 3D mock-ups and the canopy was divided into 20 cm cubic voxels as described in the above canopy structural section. Then, radiation transfer through the canopy was computed by considering Beer's law (Ross 1981) for light beam penetration into a turbid medium in each voxel. The computation of Ac and Ec was based on the Jarvis (1976) and Farquhar (1980) sub-models, respectively. Meteorological datafiles and leaf physiology-related parameters were obtained from Yang (2016), where all the parameters were measured and estimated from dwarf M26 interstock 'Fuji' trees grafted on a vigorous *Malus micromalus* rootstock. The 'Fuji' trees were planted in an apple orchard 30 km away from the apple orchard in this study.

Data analysis

The TLA, PLA, STAR, and V data were analyzed for the whole canopy and each shoot type, and LAD, ζ, PEA, MOD, and μ data were analyzed for the whole canopy. Therefore, all the variables were analyzed combining the 2 years with two-way ANOVA including cultivar and year factors and their interaction. Before two-way ANOVAs were conducted, variables were analyzed to ensure data were normally distributed and the variances were homogeneous based on the *Shapiro.test* and *Bartlett.test*, respectively. Significant differences among treatments were distinguished by different letters using Duncan's multiple mean comparison test at $p < 0.05$. Differences between training systems in the STAR distributions of voxels and shoots and LAD distributions of voxels for whole trees and each shoot type were analyzed using a non-parametric Chi-square test. All data

were analyzed using the R software, with agricolae and stats packages (R Development Core Team 2019).

Results

Tree-scale canopy structure

Between years, canopy V was 51% higher and TLA was 37% higher in the year 2017 compared to 2016 (Fig. 1, Table 2). The increase in canopy V between years occurred within the canopy above a height of 1 m. The LAD in the year 2017 was significantly lower than that in year 2016. Bi-axis training had a significantly lower LAD than single-axis training. LAD_{var} was affected by year rather than training.

All the trees showed a LAD gradient from the outer periphery to the inner canopy in both years (Fig. 2). There were fewer zones with LAD values greater than 3 in bi-axis trees than in single-axis trees. This difference was significant in the year 2016 (30% in bi-axis and 39% in single-axis trees to the total voxel number) but was not significant in the year 2017 (both 31% relative to the total voxel number).

Intra-tree scale canopy structure

In bi-axis trees, differences in leaf area among the three shoot types were not significant, irrespective of the year (Table S3). In single-axis trees, VL had the largest TLA, followed by VS and then FS in the year 2016 and then by FS and then VS in 2017 (Table S3). The TLA values of FS and VL were significantly higher in 2017 than 2016 (Table 3). Bi-axis trees had significantly higher TLAs of FS and lower

Table 2 Information of canopy architectural and light interception traits at tree-scale estimated from isolated 3D virtual plants for 'Fuji' trees trained either with a bi-axis or single-axis training system in 2016 and 2017, respectively

Year	Training system	V	TLA	LAD	LAD_{var}	PLAi	PEA	STARi	MOD	μ	Po
Mean per year											
2016		1.44	4.07	2.84	2.60	1.71	4.93	0.42	0.82	0.62	0.65
2017		2.24	5.75	2.56	2.03	2.41	6.40	0.42	0.89	0.63	0.62
p values		**0.0023**	**0.0169**	**0.0144**	**0.0464**	**0.0067**	**0.0088**	0.9581	0.1146	0.456	**0.0308**
Mean per training system											
Bi-axis		1.79	4.52	2.53	2.24	1.90	5.67	0.42	0.79	0.62	0.66
Single-axis		1.98	5.54	2.87	2.43	2.26	5.81	0.40	0.95	0.63	0.61
p values		0.5366	0.1559	**0.0037**	0.3860	0.2360	0.9993	0.0801	**0.0082**	0.676	**0.0113**
Mean per training system × year											
2016	Bi-axis	1.42b	3.66b	2.57b	2.67	1.60b	4.86b	0.43	0.74b	0.62	0.67a
	Single-axis	1.47b	4.69ab	3.19a	2.74	1.90ab	5.06ab	0.40	0.93a	0.62	0.63bc
2017	Bi-axis	2.15a	5.39a	2.50b	1.82	2.24a	6.48a	0.42	0.83b	0.62	0.64ab
	Single-axis	2.32a	6.11a	2.62b	2.23	2.51a	6.32a	0.40	0.96a	0.64	0.60c
p values		0.7454	0.7809	**0.0176**	0.5488	0.8023	0.6693	0.3176	0.6112	0.434	0.6700

Means followed by different letter in each column are significantly different at $p \leq 0.05$. For abbreviations, see the list in Table 1

The *p* values in bold are significant at $p < 0.05$

Fig. 2 Leaf area density (LAD, $m^2\ m^{-3}$) spatial distribution as a function of tree height above ground surface and distance to tree trunk based on virtual isolated trees for 'Fuji' trained either with a bi- or single-axis training systems in 2016 and 2017, respectively. The dashed line represents the central primary axis for single-axis trees and the 'virtual' middle parallel line between two primary axes for bi-axis trees
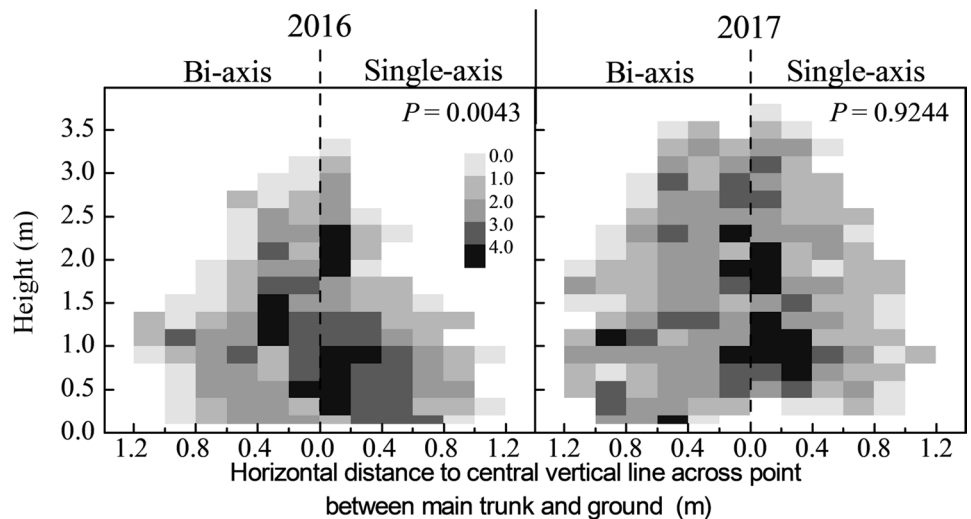
TLAs of VL than single-axis trees. TLAs of VLs of bi-axis training trees were approximately 60% those of single-axis trees, irrespective of year.

In 2016, VL was higher and more widely distributed within canopy than VS and FS; the latter two were distributed beneath a height of 2.0 m and showed a similar spatial distribution (Fig. 3). In 2017, VS and FS had a higher and wider distribution within the canopy as compared to their distribution in the previous year, irrespective of the training systems. In the year 2016, the FS of bi-axis trees had significantly more zones with LAD values > 3 than the FS of single-axis trees (24% for bi-axis and 15% for single-axis trees relative to the total voxel number), but had significantly fewer zones with LAD > 2 for VS (30% for bi-axis and 50% for single-axis trees relative to the total voxel number) and

VL (28% for bi-axis and 41% for single-axis trees relative to the total voxel number). However, in 2017, there were significantly fewer zones with LAD values > 2 for VL in bi-axis trees than single-axis trees (7% for bi-axis and 18% for single-axis trees relative to the total voxel number), and LAD distribution of the VS and FS was similar between the two training systems.

Tree-scale light interception of isolated trees

When averaged over years, year 2017 had significantly greater PLA and PEA values, than year 2016 (Table 2). Bi-axis trees had significantly lower MOD and higher Po values than single-axis trees, irrespective of training system or year. STAR was also unaffected either by year or training system.

Table 3 Total leaf area (TLA, m^2), projected leaf area (PLA, m^2) and silhouette to total area ratio (STAR) of fruiting shoot (FS), vegetative short shoot (VS) and vegetative long shoot (VL) estimated from iso- lated 3D virtual plants for 'Fuji' trees trained either with a bi-axis or single-axis training system in 2016 and 2017, respectively

Year	Training system	FS			VS			VL		
		TLA	PLAi	STARi	TLA	PLAi	STARi	TLA	PLAi	STARi
Mean per year										
2016		1.22	0.48	0.40	1.33	0.40	0.31	1.66	0.87	0.53
2017		1.95	0.76	0.39	1.37	0.41	0.30	2.43	1.18	0.49
p values		**0.0156**	**0.0112**	0.6430	0.8717	0.8704	0.3467	**0.0195**	**0.0286**	**0.0022**
Mean per training system										
Bi-axis		1.74	0.68	0.39	1.28	0.43	0.34	1.50	0.80	0.53
Single-axis		1.43	0.56	0.39	1.42	0.39	0.27	2.58	1.25	0.49
p values		**0.0398**	0.1937	0.9510	0.5501	0.5191	**0.0005**	**0.0036**	**0.0114**	**0.0006**
Mean per training system × year										
2016	Bi-axis	1.52ab	0.60ab	0.40	0.88	0.30c	0.34a	1.25b	0.67b	0.54a
	Single-axis	0.91b	0.36b	0.39	1.78	0.50b	0.28b	2.07b	1.06ab	0.51a
2017	Bi-axis	1.95a	0.75a	0.39	1.67	0.56a	0.34a	1.76b	0.92b	0.52a
	Single-axis	1.94a	0.76a	0.39	1.07	0.27c	0.25b	3.09a	1.44a	0.46b
p values		0.2415	0.1894	0.7350	**0.0128**	**0.0060**	0.3667	0.3519	0.6659	0.0790

Different letters within a column are significantly different at $p \leq 0.05$

The *p* values in bold are significant at $p < 0.05$

Tree-scale STAR spatial distributions of the canopies were drawn as a function of voxel distance to tree height and to the central primary axis for single-axis trees and to the 'virtual' middle parallel line between two primary axes in bi-axis trees (Fig. 4). The STAR declined gradually from the top to the base and from the periphery to the inner canopy in both 2016 and 2017. Irrespective of year, there were few zones with STAR < 0.15 (0.12–0.87% relative to the total voxel number). In both years, bi-axis trees had more zones within the canopy with STAR > 0.3 compared with single-axis trees (92% and 90% for bi-axis trees in 2016 and 2017, respectively, and 83% in both years for single-axis trees relative to the total voxel number). Consistent with the STAR spatial distribution, bi-axis trees had significantly fewer shaded shoots and more shoots with STAR values > 0.30, regardless of year (67% and 62% relative to the total shoot number for bi-axis trees in 2016 and 2017, respectively, with corresponding values of 54% and 44%, respectively, for single-axis trees) (Fig. 5). Between years, the proportion of shoots with STAR < 0.15 in bi-axis trees from the year 2016 to 2017 decreased from 5 to 4%. However, the proportion of shoots with the STAR < 0.15 in single-axis trees from the year 2016 to 2017 increased from 8 to 16%.

Intra-tree light interception of isolated trees

Among shoot types, the mean STAR of the VL (range 0.46–0.55; mean 0.51) was greater than the FS (range 0.34–0.44; mean 0.39) and VS (range 0.23–0.36; mean 0.30), and the mean STAR of FS was greater than VS (Table S3).

From the year 2016 to 2017, the PLA of the FS increased and the STAR of VL decreased significantly (Table 2). When averaged over the training systems, the bi-axis trained trees had significantly lower PLA of VL as compared to single-axis trees, but their STAR was greater than that of single-axis trees.

Among shoot types, VL had more even STAR spatial distribution than the FS and VS, with few voxels having STAR values < 0.30 (Fig. 6). The STAR distributions in bi-axis trained trees were significantly improved for all three shoot types compared to single-axis trees, with fewer voxels with STAR values < 0.3 and more voxels with STAR > 0.3, regardless of year. Consequently, significantly more shoots in bi-axis trees had higher light interception compared to single-axis trees, irrespective of shoot type (Fig. 7).

Light interception in virtual orchards

The STARo values in virtual orchards were lower than the STAR values of isolated trees, regardless of the whole can- opy or each shoot type (Tables 2, 3 and 4). For the whole canopy and all shoot types (except STARo of VS), the STARo values were significantly higher and the Lms values were significantly lower in 2016 than in 2017 (Table 4). The whole canopy and VS and VL had similar Lms values in the

Fig. 3 Leaf area density (LAD, $m^2\ m^{-3}$) spatial distribution as a function of tree height above ground surface and distance to tree trunk for fruiting shoot (FS), vegetative long shoot (VL) and vegetative short shoot (VS) based on virtual isolated trees for 'Fuji' trained either with a bi- or single-axis training systems in 2016 and 2017, respectively
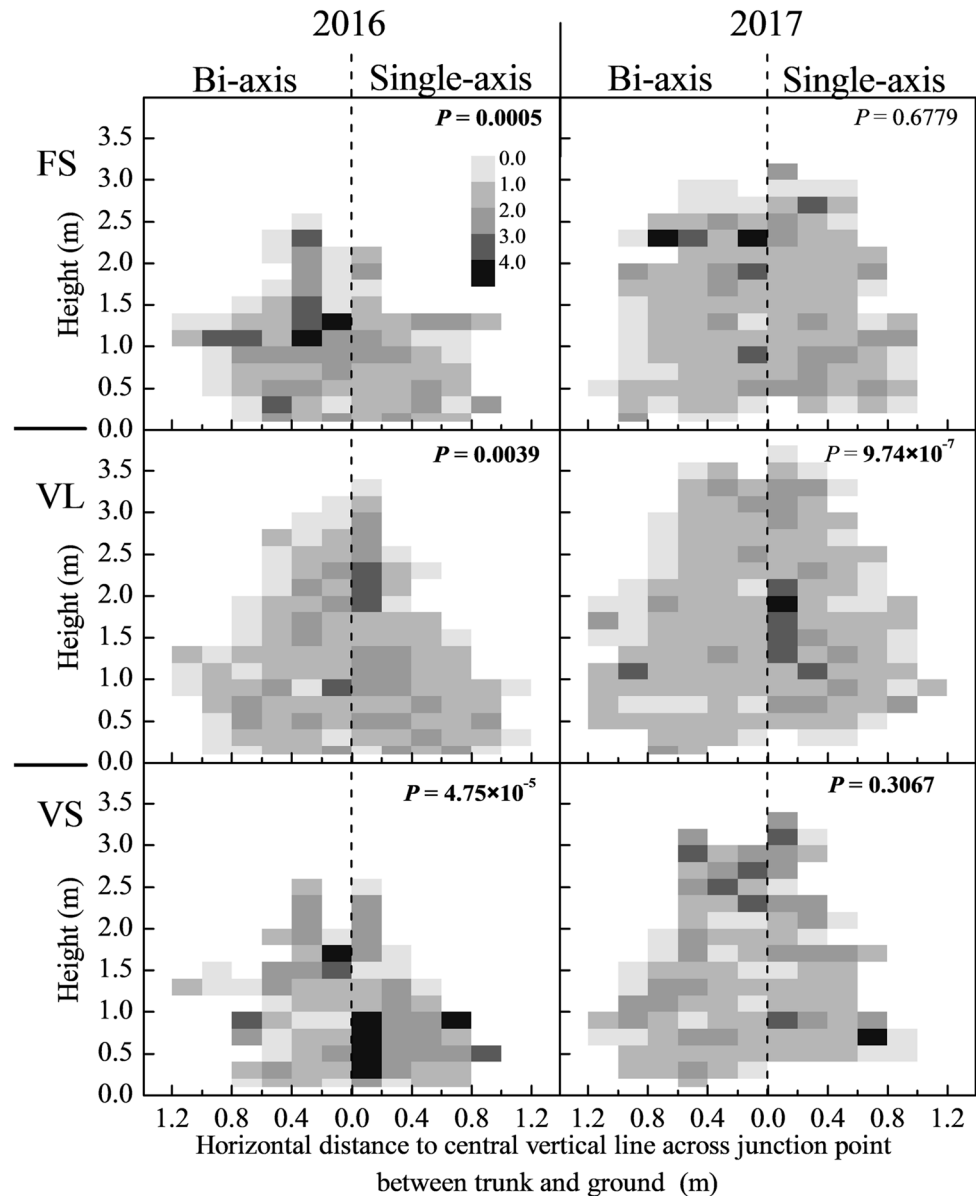
two training systems. However, the Lms of FS in bi-axis trees was 11% lower than that in single-axis trees. On average, the STARo for VS and VL in bi-axis trees were 25% and 10% greater, respectively, than that in single-axis trees.

Tree-scale photosynthesis, transpiration, and water use efficiency of isolated canopy

When averaged over year, no significant differences in Ac, Ec, and WUEc were found (Table 5). However, the mean values of Ac in bi-axis trained trees were 26% higher than those in single-axis trees, and a similar significant increasing trend was found in each year between the two training systems. The mean Ec for both training systems was similar,

leading to a significantly higher WUEc in bi-axis than in single-axis trees.

Discussion

The present study illustrated the interest in using 3D virtual plants to study the impact of bi-axis training on canopy architecture, light interception, and photosynthetic rate (Marshall-Colon et al. 2017). The combined method of using partial 3D digitizing and random sampling enabled us to describe the detailed 3D structure of trees and extract canopy structure and light interception parameters and their spatial distributions both for whole trees and each type of shoot (Sonohat et al. 2006), considering the shading effect
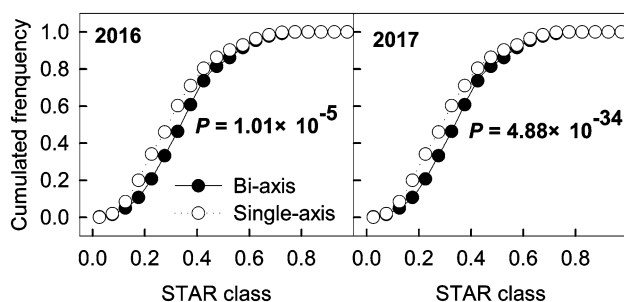
Fig. 4 Silhouette to total area ratio (STAR) spatial distribution as a function of tree height above ground surface and distance to tree trunk based on virtual isolated trees for 'Fuji' trained either with a bi- or single-axis training system in 2016 and 2017, respectively
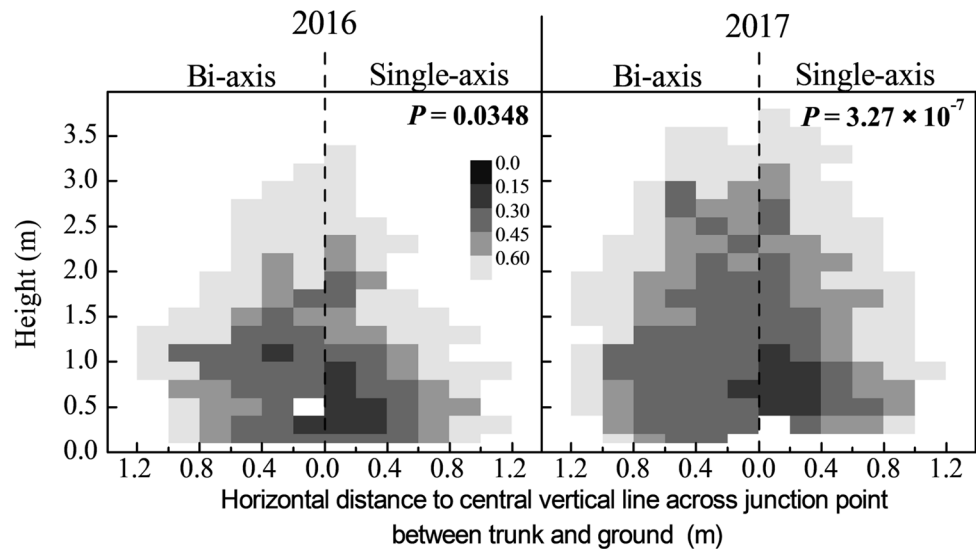
from the neighboring trees. The generation of 3D virtual plants from ruler grammar simulation is random and cannot fully represent the tree status in field (Da Silva et al. 2013, 2014). Laser scanning usually misses small sized shoots (Pallas et al. 2018), but with 3D digitizing, all shoots and types can be fully and precisely described.

Bi-axis training effects on canopy structure and light partitioning among shoots of isolated trees

Based on the detailed 3D virtual plant (Fig. 1), isolated tree STAR and its components (PLA, PEA, MOD, Po, and μ) (Nilson 1971; Smolander et al. 1994; Sinoquet et al. 2007) were quantified in the present study. A better illuminated canopy was characterized by higher STAR and accompanied by a higher Po and μ, and a lower MOD (Sinoquet et al. 2007; Duursma et al. 2012). The light interception components are functions of structural properties of canopy. Both the year and training systems affected the canopy properties, such as tree size, leaf area, shoot composition, and their spatial distribution.


Fig. 5 Silhouette to total area ratio (STAR) distribution of all shoots based on virtual isolated trees for 'Fuji' trained either with a bi- or single-axis training systems in 2016 and 2017, respectively

Regarding the year effect, TLA, V, LAD, and LAD_{var} were significantly different between the years (Table 2). Under most conditions, smaller trees (based on V) and lower LAD and LAD_{var} benefited the light penetration into canopy. However, the light interception components (based on Po) were not improved by the decrease in the LAD and LAD_{var} in the year 2017. This is consistent with a previous study where a large database of 1831 3D virtual plants was used and the results showed that trees with the same LAD could have totally different STAR values (Duursma et al. 2012). This may be because that trees have similar canopy structural parameters at the tree scale, but their spatial arrangement of leaves is different. Therefore, we suggest that changes in the PLA, PEA, and Po could be due to the increase in canopy TLA and V from year 2016 to 2017 and the optimized spatial distribution of leaves. Sinoquet et al. (2007) also showed that increased tree size and leaf area decreased the light interception efficiency. For each training system, the same leaf and shoot allometric relationships were used between years. As genotype, rootstock, and horticultural practices were identical between the two training systems, the climate, tree ontogeny, and increased shading within canopy in consecutive years may affect the shoot- and leaf-scale allometric relationships by affecting leaf size and growth duration and number of leaves per shoot (Chen et al. 2019). Therefore, the effect of year on tree architecture could be underestimated. If responses of shoot and leaf development to climate, tree ontogeny and shading between two training systems were not identical, the training effect could be underestimated, and this needs further study.

Accordingly, the significant improvement in the canopy MOD and Po by the application of the bi-axis training system to the apple trees might be the result of both the reduction in LAD and its spatial distribution (Table 2 and Figs. 2 and 3). Particularly, when compared to the spatial

Fig. 6 Silhouette to total area ratio (STAR) spatial distribution as a function of tree height above ground surface and distance to tree trunk for fruiting shoot (FS), vegetative long shoot (VL) and vegetative short shoot (VS) based on virtual isolated trees for 'Fuji' trained either with a bi- or single-axis training systems in 2016 and 2017, respectively
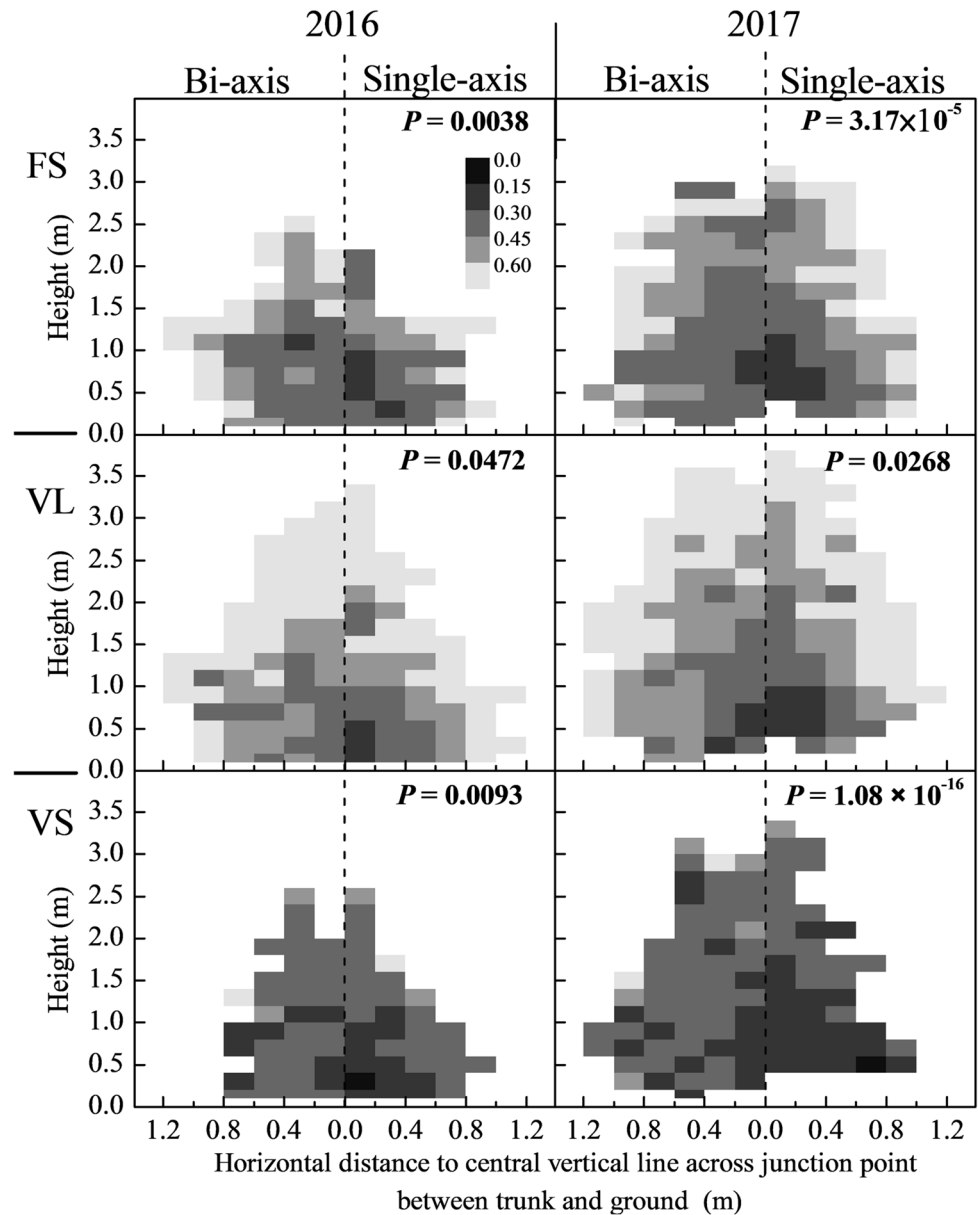
distributions of the STAR and the STAR of individual shoots between the training systems, light was more evenly distributed and more shoots had higher light interception efficiency with bi-axis training (Figs. 4, 5, 6 and 7). However, the averaged STAR value of isolated trees was not affected by the training systems. Therefore, the bi-axis training effect on canopy light interception performance evaluated by the STAR of isolated trees might be underestimated because of lack of knowledge of the heterogeneity of light within the canopy. The spatial distribution of LAD for a whole tree was decomposed into shoot types (Fig. 3). In both years, the lower proportions of VL and more uniform LAD spatial distribution of VL in bi-axis than in single-axis trained trees contributed to the improvement of light interception.

As the VLs are extension shoots, they are net carbon sinks in the early season and only a few of the fixed assimilates are exported to other shoots and fruits in the mid- and late season (Johnson and Lakso 1986a, b; Lauri and Kelner 2001). A lower proportion of VL (Fig. S3) and lower leaf area of VL in bi-axis training suggested that the fruit growth in bi-axis trees had less carbon competition from vegetative growth of VL compared to single-axis trees, which have more VL. This suggested lower tree vigor in bi-axis trees, which was also validated by a smaller annual trunk cross-sectional area compared to single-axis trees (Musacchi 2008b; Ma et al. 2020). The reduction of TLA in bi-axis trees (Table 2) may result from the higher frequency of bourse shoots (Fig. S3), which have lower shoot leaf number and shoot leaf area compared to single-axis trees (Table S1). 'Fuji' trees usually
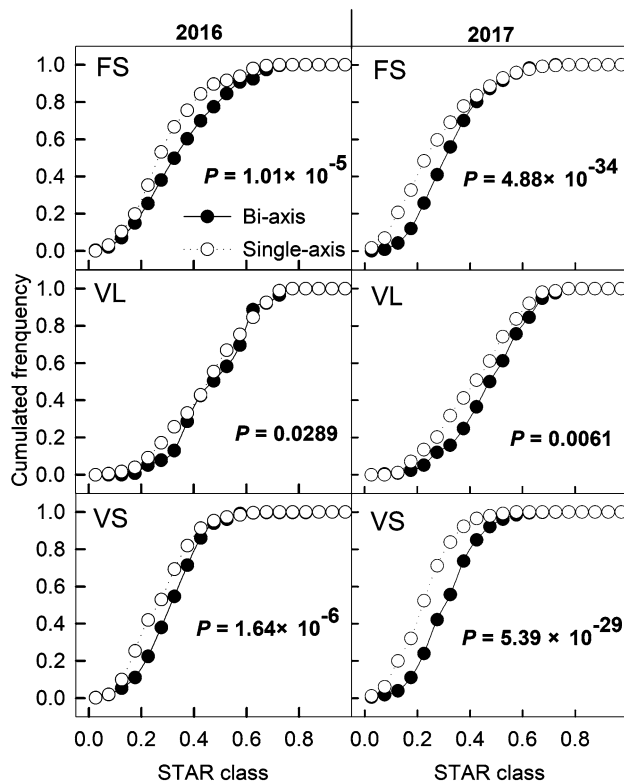
Fig. 7 Silhouette to total area ratio (STAR) distribution of fruiting shoots (FS), vegetative long shoots (VL) and vegetative short shoots (VS) based on virtual isolated trees for 'Fuji' trained either with a bi- or single-axis training systems during 2016 and 2017, respectively

have strong vegetative growth due to high precipitation during late summer and autumn on the Chinese Loess Plateau, which leads to higher biennial bearing and a higher labor need for pruning (Han et al. 2008; Xing et al. 2016). Therefore, bi-axis training could help reduce the biennial bearing and required labor for 'Fuji' trees by reducing the tree vigor and improving the light environment within the canopy.

Among shoot types, the VL had the highest STAR, followed by FS and VS, regardless of the year, training system and the effect of neighboring trees (Tables 3 and 4 and S3 and Fig. 6). The light interception of each shoot type was in accordance with its spatial distribution and STAR values of individual shoots. The light interception partitioning among shoot types and their spatial distribution were consistent with the reported patterns in apple trees (Stephan et al. 2008; Yang et al. 2016). The STAR values of FS and VS were lower than the STAR of the whole tree, irrespective of the year and training, indicating that FS and VS were in shaded areas. The difference in the light interception among shoot types was closely related to their spatial distribution of LAD. The distribution of VL was the outermost, that of VS was the innermost, with FS intermediate between. Moreover, VLs have a longer internode length in favor of light interception (Takenaka 1994; Niinemets et al. 2005). Although the STAR of FS at the tree scale was not improved by bi-axis training as compared to single-axis training, the STAR spatial distribution of FS was significantly improved, including VL and VS. These led to a cumulative effect on the trees subjected to bi-axis training, allowing more light penetration into the canopy and reducing the inner shading compared to single-axis tall spindle trees, particularly for the FS and VS.

Table 4 Silhouette to total area ratio (STARo) estimated from 3D plants in a virtual orchard and light mutual shading (Lms) estimated from difference of STAR between isolated trees and trees in virtual orchard for the whole canopy, fruiting shoot (FS), vegetative long shoot (VL) and vegetative short shoot (VS) in 'Fuji' trees trained either with a bi-axis or single-axis training system in 2016 and 2017, respectively

Year	Training system	Whole tree		FS		VS		VL	
		STARo	Lms	STARo	Lms	STARo	Lms	STARo	Lms
Mean per year									
2016		0.34	0.19	0.31	0.22	0.24	0.22	0.44	0.16
2017		0.30	0.25	0.27	0.31	0.22	0.27	0.38	0.24
p values		**0.0189**	**0.0089**	**0.0388**	**0.0031**	0.1522	**0.0443**	**0.0016**	**0.0210**
Mean per training system									
	Bi-axis	0.33	0.22	0.29	0.25	0.26	0.24	0.43	0.20
	Single-axis	0.31	0.22	0.28	0.28	0.21	0.25	0.39	0.21
P values		0.0976	0.5680	0.3746	**0.0192**	**0.0055**	0.6079	**0.0051**	0.0954
Mean per training system × year									
2016	Bi-axis	0.35a	0.19	0.32	0.20b	0.27a	0.22	0.45a	0.17b
	Single-axis	0.32ab	0.21	0.29	0.27ab	0.22ab	0.26	0.43a	0.20ab
2017	Bi-axis	0.31ab	0.26	0.27	0.29a	0.25a	0.27	0.41a	0.23ab
	Single-axis	0.30b	0.27	0.26	0.32a	0.19b	0.27	0.34b	0.25a
p values		0.3138	0.7418	0.4524	0.1369	0.5377	0.0959	0.1369	0.4966

Different letters within a column are significantly different at $p \leq 0.05$. For abbreviations, see the list in Table 1

The *p* values in bold are significant at $p < 0.05$

Table 5 Canopy net photosynthetic rate (Ac), transpiration rate (Ec) and water use efficiency (WUEc) estimated from RATP model based on isolated 3D virtual plants in 'Fuji' trees trained either with a bi-axis or single-axis training system in 2016 and 2017, respectively

Year	Training system	Ac (mmol CO_2 m^{-2} day^{-1})	Ec (mol H_2O m^{-2} day^{-1})	WUE$_c$ (mmol CO_2 mol^{-1} H_2O)
Mean per year				
2016		166.88	132.20	1.32
2017		172.39	149.00	1.18
p values		0.293	0.166	0.2409
Mean per training system				
	Bi-axis	189.38	142.53	1.38
	Single-axis	149.89	138.68	1.13
p values		**< 0.001**	0.745	**0.0406**
Mean per training system × year				
2016	Bi-axis	185.84a	135.20	1.44a
	Single-axis	147.91b	129.20	1.20ab
2017	Bi-axis	192.92a	149.86	1.32ab
	Single-axis	151.87b	148.15	1.05b
p values		0.764	0.856	0.8966

Different letters within a column are significantly different at $p \leq 0.05$

The *p* values in bold are significant at $p < 0.05$

Mutual shading effect on light partitioning among shoots in a virtual orchard

Apart from the year and training effect, the planting density in the orchard plays an important role in the determination of the light interception efficiency (Trentacoste et al. 2015). Depending on the density, a non-negligible portion of branches may penetrate the neighboring trees in the same row. Consequently, the STAR values of trees in the virtual orchard were lower than those of the isolated trees in current study, and the difference between years or training systems were exaggerated, irrespective of tree- or intra-tree scales. The virtual orchard setting made the in silico experiment more realistic as the trees were planted as they were in a real orchard. Our virtual experiment highlighted the important shading effect due to neighboring trees which could reduce the STAR of trees in virtual orchard with a range of 12–34% compared to the STAR of isolated trees. This suggested that potential improvement of shaded leaves could be an option to enhance the canopy light use efficiency (Song et al. 2013). When the planting density of single-axis trees increased from 1.2 × 3.5 to 1.0 × 3.5 m, the differences in light mutual shading between the two training systems were significant, irrespective of the tree- or intra-tree scales (Table S2). This revealed that increased planting density will lead to more shading within the canopy, and a virtual orchard could be a way to optimize planting density. However, the single-axis trees were digitized in a planting density of 1.0 × 3.5 m.

When these trees were planted in lower planting density (1.2 × 3.5 m), their LAD and crown development may be different from trees in higher planting densities due to different shading by neighboring trees. Except for FS, bi-axis trained trees had similar mutual shading to single-axis trees for both tree and vegetative shoots under the same planting density (Table 4). However, the vegetative shoots of bi-axis trees had significantly higher STARs. Thus, based on the STAR of the isolated trees or trees in the virtual orchard, the light interception efficiency of bi-axis trees improved by decreasing LAD and optimizing the spatial distribution of LAD at a tree scale rather than by limiting the mutual shading at the orchard scale. The VL had the lowest mutual shading, and VS and FS had similar mutual shading (Tables 4 and S2–3). This difference may also be related to their spatial distribution as discussed earlier.

Bi-axis training effect on photosynthetic rate of isolated canopy

A light intensity of at least 25–30% within canopy is required for continual flowering and high-quality apple fruits (Jackson 1980). The positive effects of bi-axis training on the fruit soluble solids, yield efficiency (Musacchi 2008b), dry matter production, flowering (van Hooijdonk et al. 2015; Ma et al. 2020), leaf gas exchange (Afonso et al. 2017), and net canopy photosynthetic rate could therefore be interpreted as a result of the significant improvement of the light interception and distribution at both the whole tree and intra-tree scale. A STAR of 0.15 is suggested to be equal to a light intensity of 30% (Yang et al. 2016). In the two training systems, only a few zones with the STAR less than 0.15 existed (Figs. 4 and 6). This could be because all the trees in the present study were at a younger stage than adult trees used in other studies (Stephan et al. 2008; Yang et al. 2017). Bi-axis training isolated trees had a 5% higher STAR compared to single-axis training. However, modeled photosynthetic rate of isolated canopy in bi-axis trees was 26% higher than single-axis trees. Therefore, the increase in the light interception cannot only interpret the increase in the photosynthetic rate. In the present study, the differences in microclimate and photosynthetic-related processes between two training systems were not considered during photosynthesis modeling. The improvements in the microclimate within the canopy and the photosynthetic-related processes induced by enhanced light interception may contribute to the increase in canopy net photosynthetic rate, such as leaf temperature, leaf nitrogen content, and maximal stomatal conductance (Woods et al. 2018; Kumarathunge et al. 2019). Early-season leaf area development in 1-year-old trees was identified as the main reason for a higher dry matter production in bi-axis trees compared to single-axis trees (van Hooijdonk et al. 2015). However, the present study suggested that

the optimized structure in bi-axis trees could be the main reason for better performance, whereas different reasons may result from the different tree ages and environmental conditions (Foster et al. 2016).

Although the canopy volume of bi-axis trees was not significantly different compared to that of single-axis trees (Table 2), the canopy of bi-axis trees occupied more space above 2 m height than single-axis trees (Figs. 1 and 2). This suggested that the thinner canopy of bi-axis trees was potentially beneficial for light penetration into the canopy (Jackson 1970) and mechanical harvesting. The bi-axis canopy design will arouse more thin 2D planar tree canopy with more scaffolds, similar to Cordon training in grapevines.

Conclusions

In general, by taking advantages of 3D virtual plant modeling, the present study showed that the bi-axis training system improved the light interception efficiency, light spatial distribution, and canopy net photosynthetic rate and reduced the tree vegetative growth compared to the single-axis training system. The two training systems had similar light interception partitioning to fruiting shoots, however, light interception partitioning to vegetative shoots increased and light mutual shading of FS decreased in bi-axis training compared to single-axis training. The light interception increased in bi-axis trees through improvement in the canopy structure by decreasing the LAD and optimizing the spatial distribution of LAD at the tree scale, particularly for vegetative long shoots. Light mutual shadings between two training systems were similar. Further studies will be conducted to evaluate the effect of bi-axis training on the canopy structure and light interception in adult apple trees, and on the variability of leaf photosynthesis and related physiological processes within the canopy.

Author contribution statement Conceptualization: MH, DZ and WY. Material preparation and data collection were performed by XM, DM, SH and JS. Data analysis were performed by WY and XM. The first draft of the manuscript was written by WY and EC and all authors commented on previous versions of the manuscript. All authors read and approved the final manuscript.

Compliance with ethical standards

Conflict of interest The authors declare that they have no conflict of interest statement.

References

Adam B, Donès N, Sinoquet H (2002) VegeSTAR–software to compute light interception and canopy photosynthesis from images of 3D digitised plants, version 4.0. UMR PIAF INRA-UBP, Clermont-Ferrand

Afonso S, Ribeiro C, Bacelar E, Ferreira H, Oliveira I, Silva A, Gonçalves B (2017) Influence of training system on physiological performance, biochemical composition and antioxidant parameters in apple tree (*Malus domestica* Borkh.). Sci Hortic 225:394–398

Barthélémy D, Caraglio Y (2007) Plant architecture: a dynamic, multilevel and comprehensive approach to plant form, structure and ontogeny. Ann Bot 99:375–407

Buler Z, Mika A (2004) Evaluation of the 'Mikado' tree training system versus the spindle form in apple trees. J Fruit Ornam Plant Res 12:49–60

Buler Z, Mika A, Treder W, Chlebowska D, Palmer J, Wunsche J (2001) Influence of new training systems of dwarf and demidwarf apple trees on yield its quality and canopy illumination. Acta Hortic 557:253–260

Carter GA, Smith WK (1985) Influence of shoot structure on light interception and photosynthesis in conifers. Plant Physiol 79:1038

Chen D, Pallas B, Martinez S, Wang Y, Costes E (2019) Neoformation and summer arrest are common sources of tree plasticity in response to water stress of apple cultivars. Ann Bot 123:877–890

Colaço AF, Molin JP, Rosell-Polo JR, Escolà A (2018) Application of light detection and ranging and ultrasonic sensors to high-throughput phenotyping and precision horticulture: current status and challenges. Hortic Res 5:35

Corelli-Grappadelli L, Lakso AN (2007) Is maximizing orchard light interception always the best choice? Acta Hortic 732:507–518

Costes E, Lauri PÉ, Regnard J (2006) Analyzing fruit tree architecture: implications for tree management and fruit production. Hortic Rev 32:1–61

Costes E, Lauri PÉ, Simon S, Andrieu B (2013) Plant architecture, its diversity and manipulation in agronomic conditions, in relation with pest and pathogen attacks. Eur J Plant Pathol 135:455–470

Coupel-Ledru A, Pallas B, Delalande M, Boudon F, Carrié E, Martinez S, Regnard J-L, Costes E (2019) Multi-scale high-throughput phenotyping of apple architectural and functional traits in orchard reveals genotypic variability under contrasted watering regimes. Hortic Res 6:1–15

Da Silva D, Han L, Costes E (2013) Light interception efficiency of apple trees: a multiscale computational study based on MAppleT. Ecol Model 290:45–53

Da Silva D, Han L, Faivre R, Costes E (2014) Influence of the variation of geometrical and topological traits on light interception efficiency of apple trees: sensitivity analysis and metamodelling for ideotype definition. Ann Bot 114:1–14

den Dulk JA (1989) The interpretation of remote sensing: a feasibility study. Disertation, Landbouwuniversiteit te Wageningen

Donès N, Adam B, Sinoquet H (2006) PiafDigit–software to drive a Polhemus Fastrak 3 SPACE 3D digitiser and for the acquisition

of plant architecture, version 1.1. UMR PIAF INRA-UBP, Clermont-Ferrand

Duursma R, Falster D, Valladares F, Sterck F, Pearcy R, Lusk C, Sendall K, Nordenstahl M, Houter N, Atwell B (2012) Light interception efficiency explained by two simple variables: a test using a diversity of small-to medium-sized woody plants. New Phytol 193:397–408

Fanwoua J, Bairam E, Delaire M, Buck-Sorlin G (2014) The role of branch architecture in assimilate production and partitioning: the example of apple (*Malus domestica*). Front Plant Sci 5:338

Farquhar GD, von Caemmerer S, Berry JA (1980) A biochemical model of photosynthetic CO_2 assimilation in leaves of C3 species. Planta 149:78–90

Feng F, Li M, Ma F, Cheng L (2014) Effects of location within the tree canopy on carbohydrates, organic acids, amino acids and phenolic compounds in the fruit peel and flesh from three apple (*Malus× domestica*) cultivars. Hortic Res 1:14019

Foster T, van Hooijdonk B, Friend A, Seleznyova A, McLachlan A (2016) Apple rootstock-induced dwarfing is strongly influenced by growing environment. J Hortic 3(2376–0354):1000180

Giuliani R, Magnanini E, Corelli-Grappadelli L (1998) Whole canopy gas exchange and light interception of three peach training systems. Acta Hortic 465:309–318

Gullo G, Motisi A, Zappia R, Dattola A, Diamanti J, Mezzetti B (2014) Rootstock and fruit canopy position affect peach [*Prunus persica* (L.) Batsch] (cv. Rich May) plant productivity and fruit sensorial and nutritional quality. Food Chem 153:234–242

Hampson CR, Quamme HA, Brownlee RT (2002) Canopy growth, yield, and fruit quality of "Royal Gala" apple trees grown for eight years in five tree training systems. HortScience 37:627–631

Han MY, Li YW, Fan CH, Zhao CP (2008) Effects of branch bending angle on physiological characteristics and fruit quality of "Fuji" apple. Acta Hortic Sin 35:1345–1350

Han L, Costes E, Boudon F, Cokelaer T, Pradal C, Silva DD, Faivre R (2012) Investigating the influence of geometrical traits on light interception efficiency of apple trees: a modelling study with MAppleT. In: Kang M, Dumont Y, Guo Y (eds) 2012 IEEE fourth international symposium on plant growth modeling, simulation, visualization and applications (PMA),. IEEE Shanghai, pp 152–159

Harley PC, Thomas RB, Reynolds JF, Strain BR (1992) Modelling photosynthesis of cotton grown in elevated CO_2. Plant Cell Environ 15:271–282

Hikosaka K, Niinemets U, Anten NP (2016) Canopy photosynthesis: from basics to applications. Springer, Dordrecht

Jackson JE (1970) Aspects of light climate within apple orchards. J Appl Ecol 7:207–216

Jackson JE (1980) Light interception and utilization by orchard systems. Hortic Rev 2:208–267

Jarvis P (1976) The interpretation of the variations in leaf water potential and stomatal conductance found in canopies in the field. Philos Trans R Soc B 273:593–610

Johnson R, Lakso A (1986a) Carbon balance model of a growing apple shoot. I: development of the model. J Am Soc Hortic Sci 111:160–164

Johnson R, Lakso A (1986b) Carbon balance model of a growing apple shoot. II: simulated effects of light and temperature on long and short shoots. J Am Soc Hortic Sci 111:164–169

Kumarathunge DP, Medlyn BE, Drake JE et al (2019) Acclimation and adaptation components of the temperature dependence of plant photosynthesis at the global scale. New Phytol 222:768–784

Larbi A, Vázquez S, El-Jendoubi H, Msallem M, Abadía J, Abadía A, Morales F (2015) Canopy light heterogeneity drives leaf

anatomical, eco-physiological, and photosynthetic changes in olive trees grown in a high-density plantation. Photosynth Res 123:141–155

Laurens F, Aranzana MJ, Arus P, Bassi D, Bink M, Bonany J, Caprera A, Corelli-Grappadelli L, Costes E, Durel CE, Mauroux JB, Muranty H, Nazzicari N, Pascal T, Patocchi A, Peil A, Quilot-Turion B, Rossini L, Stella A, Troggio M, Velasco R, van de Weg E (2018) An integrated approach for increasing breeding efficiency in apple and peach in Europe. Hortic Res 5:11

Lauri PÉ, Kelner JJ (2001) Shoot type demography and dry matter partitioning: a morphometric approach in apple (*Malus domestica*). Can J Bot 79:1270–1273

Lauri PÉ, Willaume M, Larrive G, Lespinasse JM (2004) The concept of centrifugal training in apple aimed at optimizing the relationship between growth and fruiting. Acta Hortic 636:35–42

Leis M, Mazzola C (2008) Apple tree named 'Fujiko'. vol US 2007/0226855 P1 Google Patents

Li KT, Lakso AN, Piccioni R, Robinson T (2003) Summer pruning reduces whole-canopy carbon fixation and transpiration in apple trees. J Hortic Sci 78:749–754

Ma X, Ma D, Shi J, Han M, Yang W, Zhang D (2020) Effect of bi-axis Bibaum tree shape on growth and bearing of young apple tree on dwarf rootstock. Acta Hortic Sinica 47:541–550

Mack J, Lenz C, Teutrine J, Steinhage VJC, Agriculture Ei (2017) High-precision 3D detection and reconstruction of grapes from laser range data for efficient phenotyping based on supervised learning. Comput Electron Agric 135:300–311

Marshall-Colon A, Long SP, Allen DK et al (2017) Crops in silico: generating virtual crops using an integrative and multi-scale modeling platform. Front Plant Sci 8:786

Massonnet C, Regnard J, Lauri PÉ, Costes E, Sinoquet H (2008) Contributions of foliage distribution and leaf functions to light interception, transpiration and photosynthetic capacities in two apple cultivars at branch and tree scales. Tree Physiol 28:665–678

Monteith JL (1977) Climate and the efficiency of crop production in Britain. Philos Trans R Soc Lond B Biol Sci 281:277–294

Moon P, Spencer DE, Moon P, Spencer DE (1942) Illumination from a non-uniform sky. Trans Illum Eng Soc 37:707–726

Musacchi S (2008a) BIBAUM®: a new training system for pear orchards. Acta Hortic 800:763–769

Musacchi S (2008b) Training systems and soil management for southern European pear orchards. Acta Hortic 772:447–457

Ngao J, Adam B, Saudreau M (2017) Intra-crown spatial variability of leaf temperature and stomatal conductance enhanced by drought in apple tree as assessed by the RATP model. Agric Forest Meteorol 237–238:340–354

Niinemets Ü (2010) A review of light interception in plant stands from leaf to canopy in different plant functional types and in species with varying shade tolerance. Ecol Res 25:693–714

Niinemets Ü, Sparrow A, Cescatti A (2005) Light capture efficiency decreases with increasing tree age and size in the southern hemisphere gymnosperm *Agathis australis*. Trees 19:177–190

Nilson T (1971) A theoretical analysis of the frequency of gaps in plant stands. Agric Meteorol 8:25–38

Pallas B, Martinez S, Simler O, Carrié E, Costes E, Boudon F (2018) Assessing T-LiDAR technology for high throughput phenotyping apple tree topological and architectural traits. In: XXX International Horticultural Congress IHC2018: international symposium on cultivars, rootstocks and management systems of 1281, pp 625–632

Palmer JW (1987) The measurement of leaf area in apple trees. J Hortic Sci 62:5–10

Palmer JW, Warrington IJ (1998) Underlying principles of successful apple planting systems. Acta Hortic 513:357–366

Perez RPA, Fournier C, Cabrera-Bosquet L, Artzet S, Pradal C, Brichet N, Chen TW, Chapuis R, Welcker C, Tardieu F (2019) Changes

in the vertical distribution of leaf area enhanced light interception efficiency in maize over generations of selection. Plant Cell Environ 42:2105–2119

Picheny V, Casadebaig P, Trépos R, Faivre R, Da Silva D, Vincourt P, Costes E (2017) Using numerical plant models and phenotypic correlation space to design achievable ideotypes. Plant Cell Environ 40:1926–1939

Poorter H, Niinemets Ü, Ntagkas N, Siebenkäs A, Mäenpää M, Matsubara S, Pons T (2019) A meta-analysis of plant responses to light intensity for 70 traits ranging from molecules to whole plant performance. New Phytol 223:1073–1105

Pradal C, Dufour-Kowalski S, Boudon F, Fournier C, Godin C (2008) OpenAlea: a visual programming and component-based software platform for plant modelling. Funct Plant Biol 35:751–760

Prusinkiewicz P (1998) Modeling of spatial structure and development of plants: a review. Sci Hortic 74:113–149

R Development Core Team (2019) R: a language and environment for statistical computing. R Foundation for Statistical Computing, Vienna, Austria. http://www.R-project.org/. Accessed Aug 2019

Reig G, Lordan J, Miranda Sazo M, Hoying SA, Fargione MJ, Hernan Reginato G, Donahue DJ, Francescatto P, Fazio G, Robinson TL (2019) Effect of tree type and rootstock on the long-term performance of 'Gala', 'Fuji' and 'Honeycrisp' apple trees trained to Tall Spindle under New York State climatic conditions. Sci Hortic 246:506–517

Robinson TL, Lakso AN (1991) Bases of yield and production efficiency in apple orchard systems. J Am Soc Hortic Sci 116:188–194

Robinson TL, Hoying SA, Reginato GH (2006) The tall spindle apple production system. N Y Fruit Q 14:21–28

Robinson TL, DeMarree AM, Hoying SA (2007) An economic comparison of five hight density apple planting systems. Acta Hortic 723:481–489

Robinson T, Hoying S, Reginato G (2008) The tall spindle planting system: principles and performance. Acta Hortic 903:571–579

Robinson T, Hoying S, Sazo MM, DeMarree A, Dominguez L (2013) A vision for apple orchard systems of the future. N Y Fruit Q 21:12–16

Ross J (1981) The radiation regime and architecture of plant stands. Springer, The Hague

Sanz R, Rosell JR, Llorens J, Gil E, Planas S (2013) Relationship between tree row LIDAR-volume and leaf area density for fruit orchards and vineyards obtained with a LIDAR 3D dynamic measurement system. Agric Forest Meteorol 171–172:153–162

Sinoquet H, Rivet P, Godin C (1997) Assessment of the three-dimensional architecture of walnut trees using digitising. Silva Fenn 31:265–273

Sinoquet H, Le Roux X, Adam B, Ameglio T, Daudet FA (2001) RATP: a model for simulating the spatial distribution of radiation absorption, transpiration and photosynthesis within canopies: application to an isolated tree crown. Plant Cell Environ 24:395–406

Sinoquet H, Sonohat G, Phattaralerphong J, Godin C (2005) Foliage randomness and light interception in 3D digitized trees: an analysis from multiscale discretization of the canopy. Plant Cell Environ 28:1158–1170

Sinoquet H, Stephan J, Sonohat G, Lauri PÉ, Monney P (2007) Simple equations to estimate light interception by isolated trees from canopy structure features: assessment with three-dimensional digitized apple trees. New Phytol 175:94–106

Smolander H, Stenberg P, Linder S (1994) Dependence of light interception efficiency of Scots pine shoots on structural parameters. Tree Physiol 14:971–980

Song Q, Zhang G, Zhu X (2013) Optimal crop canopy architecture to maximise canopy photosynthetic CO_2 uptake under elevated CO_2—a theoretical study using a mechanistic model of canopy photosynthesis. Funct Plant Biol 40:109–124

Sonohat G, Sinoquet H, Kulandaivelu V, Combes D, Lescourret F (2006) Three-dimensional reconstruction of partially 3D-digitized peach tree canopies. Tree Physiol 26:337–351

Stephan J, Sinoquet H, Donès N, Haddad N, Talhouk S, Lauri PÉ (2008) Light interception and partitioning between shoots in apple cultivars influenced by training. Tree Physiol 28:331–342

Strauss S, Lempe J, Prusinkiewicz P, Tsiantis M, Smith RS (2020) Phyllotaxis: is the golden angle optimal for light capture? New Phytol 225:499–510

Takenaka A (1994) Effects of leaf blade narrowness and petiole length on the light capture efficiency of a shoot. Ecol Res 9:109–114

Tang L, Yin D, Chen C, Yu D, Han W (2019) Optimal design of plant canopy based on light interception: a cases study with Loquat. Front Plant Sci 10:364

Trentacoste ER, Connor DJ, Gómez-del-Campo M (2015) Row orientation: applications to productivity and design of hedgerows in horticultural and olive orchards. Sci Hortic 187:15–29

Tustin DS, Cashmore WM, Bensley RB (1998) The influence of orchard row canopy discontinuity on irradiance and leaf area distribution in apple trees. J Hortic Sci Biotechnol 73:289–297

van Hooijdonk BM, Tustin DS, Dayatilake D, Oliver M (2015) Nursery tree design modifies annual dry matter production of newly grafted 'Royal Gala' apple trees. Sci Hortic 197:404–410

van Hooijdonk BM, Tustin DS, Oliver MJ, Dayatilake GA (2016) Leaf area development and dry matter production of newly grafted monoaxis and biaxis apple trees. Acta Hortic 1130:335–340

Wagenmakers PS, Callesen O (1995) Light distribution in apple orchard systems in relation to production and fruit quality. J Hortic Sci 70:935–948

Willaume M, Lauri PÉ, Sinoquet H (2004) Light interception in apple trees influenced by canopy architecture manipulation. Trees 18:705–713

Woods HA, Saudreau M, Pincebourde S (2018) Structure is more important than physiology for estimating intracanopy distributions of leaf temperatures. Ecol Evol 8:5206–5218

Wunsche J, Lakso AN (2000) The relationship between leaf area and light interception by spur and extension shoot leaves and apple orchard productivity. HortScience 35:1202–1206

Xing L, Zhang D, Zhao C, Li Y, Ma J, An N, Han M (2016) Shoot bending promotes flower bud formation by miRNA-mediated regulation in apple (*Malus domestica* Borkh.). Plant Biotechnol J 14:749–770

Yang W (2016) Studying the planting system and water stress effects on apple tree architecture and function with digitizing modelling. Dissertation. Northwest A&F University.

Yang W, Chen X, Saudreau M, Zhang X, Zhang M, Liu H, Costes E, Han M (2016) Canopy structure and light interception partitioning among shoots estimated from virtual trees: comparison between apple cultivars grown on different interstocks on the Chinese Loess Plateau. Trees 30:1723–1734

Yang W, Chen X, Zhang M, Gao C, Liu H, Saudreau M, Costes E, Han M (2017) Light interception characteristics estimated from three-dimensional virtual plants for two apple cultivars and influenced by combinations of rootstocks and tree architecture in Loess Plateau of China. Acta Hortic 1160:245–252

Zhu X, Long SP, Ort DR (2010) Improving photosynthetic efficiency for greater yield. Annu Rev Plant Physiol 61:235–261

Authors and Affiliations

Weiwei Yang[1,2] · Xiaolong Ma[1] · Doudou Ma[1] · Jidong Shi[3] · Sayed Hussain[5] · Mingyu Han[1] · Evelyne Costes[4] · Dong Zhang[1]

[1] College of Horticulture, Northwest A&F University, No.3 Taicheng Road, Yangling 712100, Shaanxi, China

[2] College of Agriculture, The Key Laboratory of Special Fruits and Vegetables Cultivation Physiology and Germplasm Resources Utilization in Xinjiang Production and Construction Group, Shihezi University, No.4 North Road, Shihezi 832003, Xinjiang, China

[3] Shaanxi Huasheng (Group) Corp. Fruit CO., Ltd. Weiyang Lake Tourism District, Xi'an 710021, China

[4] UMR AGAP, SupAgro, CIRAD, Equipe 'Architecture et Fonctionnement des Especes Fruiteres', University of Montpellier, INRAE, TA A 108/03, Avenue Agropolis, 34398 Cedex 05 Montpellier, France

[5] Department of Horticulture, Garden Campus, Abdul Wali Khan University Mardan (AWKUM), Mardan, Pakistan